ISSN 1070-3632, Russian Journal of General Chemistry, 2015, Vol. 85, No. 9, pp. 2167–2173. © Pleiades Publishing, Ltd., 2015.

# Reversible Optical Switching of Dirac Point of Graphene Functionalized with Azobenzene[1]

**Deepshikha**

*Center for Nanochemistry, Beijing National Laboratory for Molecular Sciences (BNLMS), State Key Laboratory for Structural Chemistry of Unstable and Stable Species, College of Chemistry and Molecular Engineering, Peking University, Beijing, PR China*
*e-mail: deepshikhasaini80@gmail.com*

Received July 29, 2014

**Abstract**—Graphene has exceptional electronic, optical, mechanical and thermal properties that determine its great potential in electronic, optoelectronic and sensing applications. In this study graphene has been covalently functionalized with azobenzene (AB) photosensitizer. The field-effect transistor (FET) with AB-functionalized graphene exhibited the p-doping effect with hole concentration ca $4 \times 10^{12}$ $cm^{-2}$ and interesting optoelectronic behaviour. The Dirac point of graphene in the FET could be controlled by light modulation due to azobenzene reversible switching between *cis* and *trans* conformations upon UV and visible light irradiation. *Cis* structure formation was initiated by UV irradiation that induced the shift of the Dirac point of graphene toward positive gate voltage. The reverse process back to *trans* form occurred under visible light irradiation or in darkness inducing the shift of the Dirac point toward negative gate voltage. The effect was reproduced repeatedly.

**Keywords:** graphene, photosensitive azobenzene, covalent modification, Raman spectroscopy, optoelectronic properties

**DOI:** 10.1134/S1070363215090224

## INTRODUCTION

Graphene-based optoelectronic devices [1–3] demonstrated clear potential in solar cells, touch screens and photodetectors [4–6]. The remarkable optical properties of graphene, including its linear optical absorption [7], tunable band-gap [8] and intrinsic photocurrent [9–12], have been demonstrated and can be integrated with its distinctive electronic and mechanical features. Weak adsorption of pristine graphene (2.3%) limits significantly its application in photodetection. Tuning of the energy level and control of electronic properties of graphene are required for electronic devices and related applications that have been explored in making graphene nanoribbon and nanomesh structures by preparing bilayer graphene and doping of graphene [13–21]. Among such approaches doping of graphene is now considered to be the easiest way to control its electrical properties. There are several approaches to the method of doping. For instance, the most common doping leads to replacing carbon atoms in graphene by nitrogen under ammonia flow at high temperature (*n*-type of doping) [19, 20]. The drawbacks of substitutional doping are low mobility and conductivity of graphene because of introduction of large number of defects into it [19–21]. Introduction of functional groups into graphene by covalent bonding also changes its electrical properties [22–24]. Formation of covalent carbon–carbon chemical bonds involving the basal plane carbon atoms presents key advantages such as high stability of the hybrid material, control over the degree of functionalization and reproducibility.

Photochromatic azobenzene has been extensively studied as a core for light-driven applications such as photoswitching [25], micropatterning [26] and reversible optical storage [27]. Azobenzene units can undergo *trans–cis* photoisomerization under UV light associated with distinctive structural rearrangements [28, 29]. Optically modulated electronic properties of carbon nanotubes (CNTs) were achieved by conformational changes of azobenzene moieties on the sidewalls. Conductance of CNTs non-covalently attached by azobenzene can be controlled by UV light due to similar transformations that lead to changes in the dipole moment of azobenzene chromophores, thus

[1] The text was submitted by the author in English.

**Table 1.** Synthesis conditions of single layer ME–GR at room temperature

| Sample | Concentration of diazonium salt, mg/mL | Reaction time, min | Stability of graphene onto substrate | Sample | Concentration of diazonium salt, mg/mL | Reaction time, min | Stability of graphene onto substrate |
|---|---|---|---|---|---|---|---|
| ME-1 | 10 | 30 | Stable | ME-6 | 10 | 30 | Stable |
| ME-2 | 10 | 60 | Stable | ME-7 | 15 | 30 | Stable |
| ME-3 | 10 | 120 | Stable | ME-8 | 20 | 30 | Stable |
| ME-4 | 10 | 240 | Stable | ME-9 | 25 | 30 | Stable |
| ME-5 | 10 | 360 | Stable | | | | |

altering the local electrostatic potential in a nanotube [30, 31]. Thus, incorporating azobenzene chromophores into graphene sheets may lead to advances in optically tunable electronic properties due to novel functional synergy. Influence of photoisomerization of azobenzene moieties on graphene is a key factor for its applications in optical and photonic devices.

In the current study azobenzene was applied as photosensitive material for graphene field effect transistors. Optoelectronic performance of the hybrid graphene-azobenzene devices was investigated. It demonstrated the defect-free *p*-doping of graphene and reversible modulation of the Dirac point in its functionalization with azobenzene via covalent bonding. *cis–trans* Reversible switch influenced the dipole moment of the molecules and hence, the extent of doping in graphene. The effects were studied by Raman spectroscopy and electrical measurements. It was possible to engineer the energy level alignment

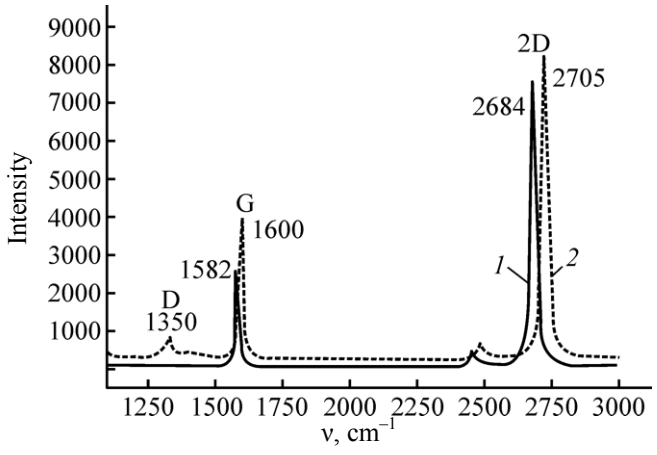


**Fig. 1**. Raman spectrum of pristine ME-graphene and azobenzene-functionalized ME-graphene. (*1*) Pristine graphene and (*2*) functialized graphene.

such as charge separation and transfer in the hybrid graphene–azobenzene systems.

## RESULTS AND DISCUSSION

The GR-AB hybrid was synthesized via covalent linkage between graphene and azobenzene justified by Raman spectroscopy (Fig. 1). The symmetric single peak of 2*D* band centred at 2684 $cm^{-1}$ was significantly more intensive than the *G* peak centred at 1582 $cm^{-1}$ indicating that graphene investigated in this study was high-quality single layer [32]. For electrodes made of ME-GR no *D* peak was detected at 1350 $cm^{-1}$, indicating that the graphene sheet was clean and defect-free. Upon functionalization the new distinctive *D* band at 1350 $cm^{-1}$ appeared. It was attributed to the covalent attachment of the functional group [33–35].

The *G* band was shifted upfield upon functionalization with azobenzene indicating the *p*-type doping of graphene. Intensity of the *D* band increased over time (Fig. 2a and Table 1) and in the presence of higher concentrations of diazonium salt (Fig. 2b and Table 1). Such result was consistent with $sp^2$ to $sp^3$ transformation of some graphene carbon atoms [36–38].

As a control experiment single layer ME-GR was treated with diazonium salt solution at room temperature for two min. Physical adsorption of the azobenzene group on GR is demonstrated by the Raman spectrum (Fig. 3) that demonstrated the characteristic signals of bands *G* (1584 $cm^{-1}$) and 2*D* (2684 $cm^{-1}$) but no signal at ca 1350 $cm^{-1}$ of *D* band. This confirmed that the functional group was adsorbed physically but not covalently on the surface of graphene.

Atomic force microscopy (AFM) was used to measure the height profiles of pristine graphene and functionalized graphene. The height for pristine single-

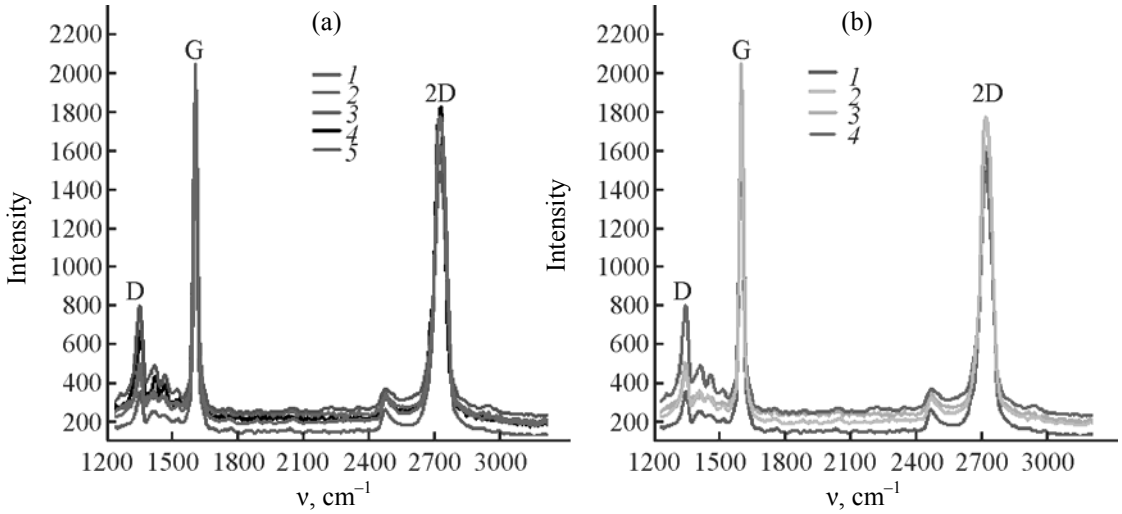


**Fig. 2.** Raman spectra of (a) ME-GR functionalized at different reaction time, min: (*1*) 30, (*2*) 60, (*3*) 120, (*4*) 240, (*5*) 360 and (b) ME-GR functionalized with different diazonium salt concentrations, mg/mL: (*1*) 10, (*2*) 15, (*3*) 20, (*4*) 25.

layer ME-GR was 0.5 nm (Fig. 4a). After chemical reaction with azobenzene diazonium solution the height of single-layer graphene increased to 1.75 nm (Fig. 4b). It indicated that the azobenzene groups were attached to the surface of graphene.

The covalent bonding of azobenzene with graphene was assessed with X-Ray Photoelectron Spectroscopy (XPS) (Figs. 4c and 4d). The C 1*s* signal observed at ca 284.5 eV broadened and decreased in intensity upon exposure to diazonium solution. The signal observed at ca 285.5 eV was attributed to the C–N bond of the azobenzene group while the decrease in the intensity of the peak at 284.5 eV was attributed to the decreased number of $sp^2$ carbon atoms in the lattice due to the change in hybridization [39–41]. The signal observed at ca. 399.3 (Fig. 4d) was assigned to the azo (–N=N–) group. AFM and XPS studies of pristine and functionalized graphene demonstrated that the azobenzene groups were attached to one side of the single-layer graphene basal plane.

We fabricated a field-effect transistor device with single-layer graphene. Graphene was mechanically exfoliated onto a 300 nm $SiO_2$/Si wafer using kish graphite by scotch tape method (Fig. 5). The graphene FET device was immersed into a solution of azobenzene diazonium salt for 24 h, followed by rinsing with acetone to remove any unbound azobenzene and then drying in the atmosphere of $N_2$.

The pristine graphene device demonstrated low *p*-type character with the Dirac point of 7.4 V (Fig. 6). AB–GR hybrid demonstrated the more pronounced *p*-type character compared to pristine graphene with the Dirac point at 13.6 V upon treatment with UV light (*trans* to *cis* isomerization) (Fig. 7a). The Dirac point upshift by 2.6 V indicated some increase of hole carriers by higher dipole moment of *cis*-azobenzene. Upon white light action (Fig. 7b) the Dirac point reverted back to ~13.6 V. Changes in the Dirac point were reversible upon alternating UV and visible light irradiation and doping level of graphene functionalized with azobenzene could be controlled. *cis* Form lowered the Fermi level while the *trans* form raised it (Fig. 7c).

Quantitative estimation of the charge carrier concentration was deduced from Dirac point shifts on

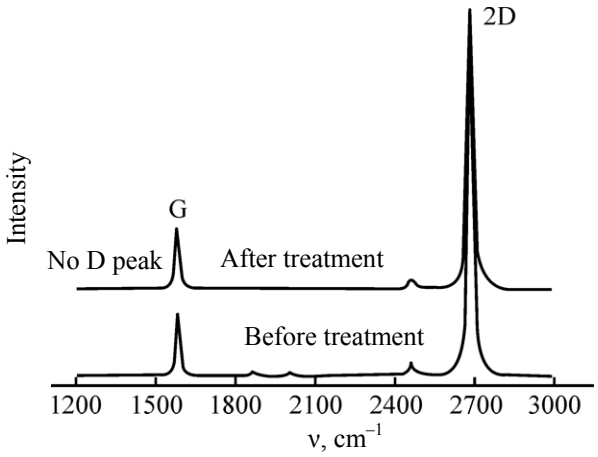


**Fig. 3.** Raman spectra of ME-GR single layer before and after chemical treatment with diazonium salt for 2 min.

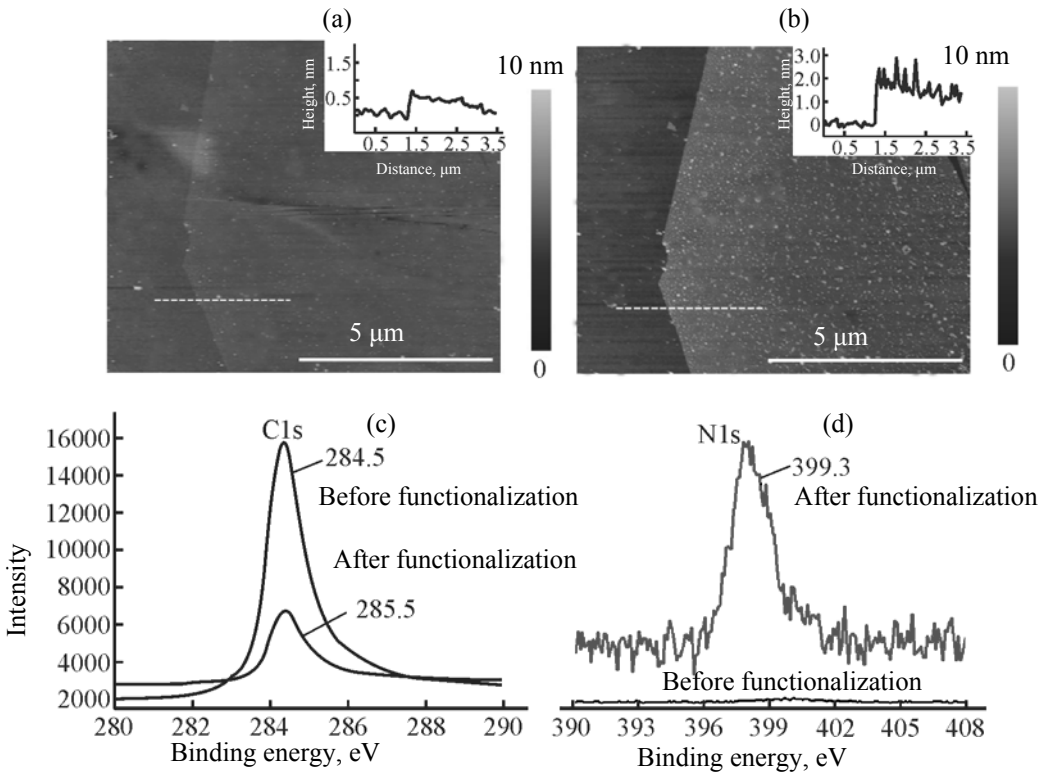


**Fig. 4.** AFM height images of (a) pristine ME-GR, (b) functionalized ME-GR, (c) C 1*s* XPS spectra of graphene before and after functionalization, and (d) N1s XPS spectra of graphene before and after functionalization.

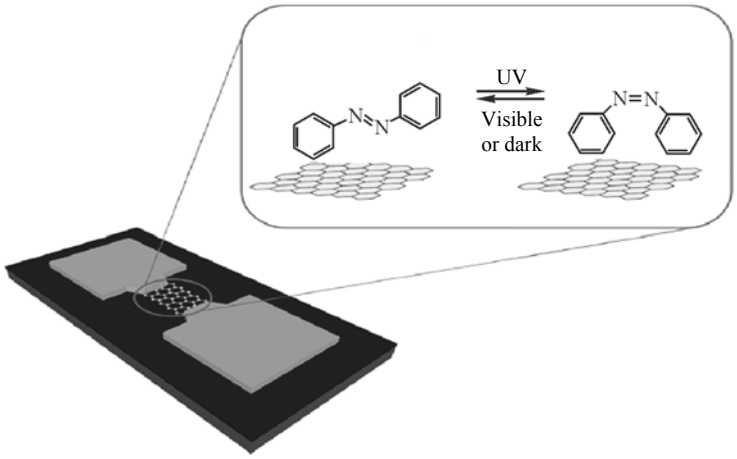


**Fig. 5.** Schematic presentation of a FET device with graphene functionalized with azobenzene.

**Table 2.** Estimated hole concentrations ($n$) deduced from Dirac point positions

| FET | Graphene | Azobenzene–graphene | UV illumination | White light illumination |
|---|---|---|---|---|
| Dirac point $V$ | 7.4 | 13.6 | 16.2 | 13.6 |
| $n \times 10^{12}$, cm$^{-2}$ | 0.0 | 4.2 | 5.1 | 4.3 |

the assumption that the very point of pristine graphene represented zero carrier concentration. Hole concentrations were derived from shifts in Dirac points (Table 2) upon functionalization, UV and white light illumination using standard charge carrier density model of Si back-gate FET:

$$n = \varepsilon_0 \varepsilon_r V_{Dirac}/eT_{OX},$$

where $\varepsilon_0$ is the permittivity of free space, $\varepsilon_r$ is the relative permittivity of $SiO_2$, $V_{Dirac}$ is the Dirac point in

voltage, $T_{OX}$ is the thickness of $SiO_2$ and e is the electron charge.

Illumination with UV light induced *trans–cis* photoisomerization and led to higher conductance resulting in upshift in the Dirac point. Reduced dipole (from *cis* to *trans*) induced by subsequent visible light illumination resulted in lower conductance and a downshift in the Dirac point. These switching events could be repeated at least over five cycles that justified stability of the system.

Graphene doping by azobenzene molecules preserved mobility of the devices. We estimated the hole mobility using the standard transistor model

$$\mu = gL/V_{SD}C_{OX}W,$$

where $g$ is the transconductance, $L$ and $W$ are the channel length and width of the device, respectively, $V_{SD}$ is the source-drain potential, and $C_{OX}$ is the gate capacitance per unit area. Pristine graphene devices demonstrated hole mobility of 1800–2000 $cm^2 V^{-1} s^{-1}$. Upon functionalization the hole mobility of azobenzene–graphene samples as well as those UV illuminated were largely preserved (1700–2000 $cm^2 V^{-1} s^{-1}$).

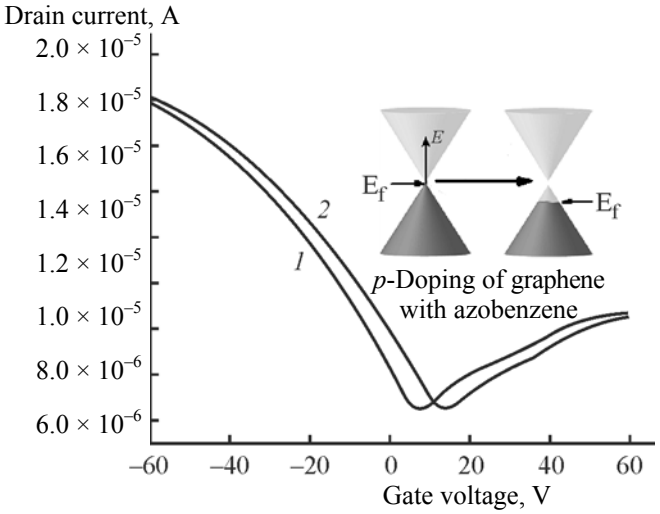


**Fig. 6.** I-Vg curves for the FET device with graphene before (*1*) and after (*2*) functionalization with azobenzene.

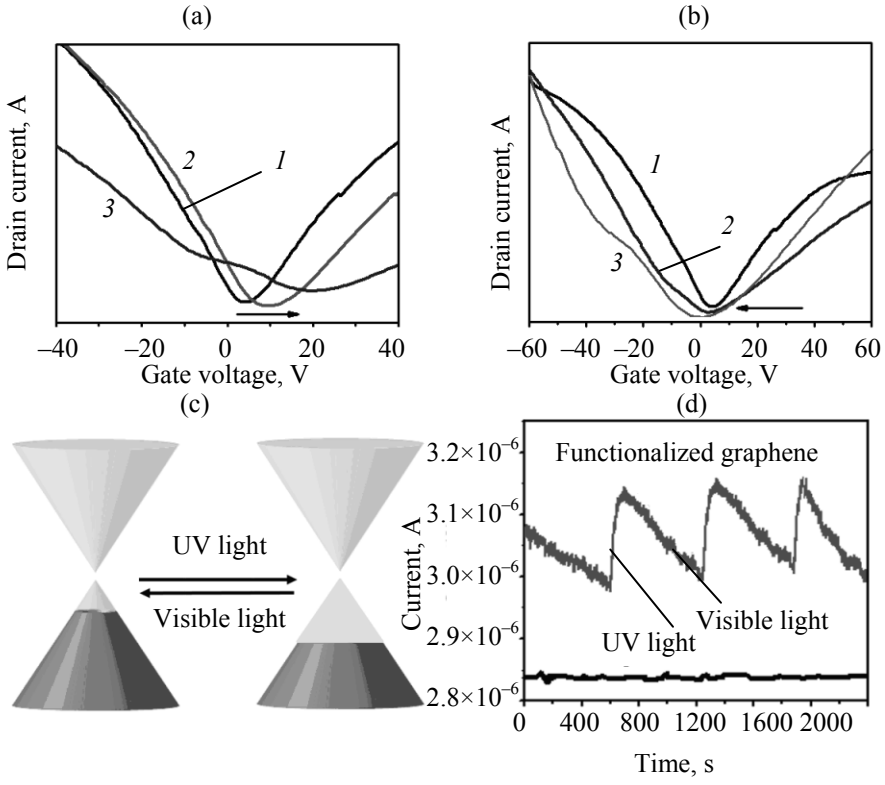


**Fig. 7.** Dirac point change in I-Vg curves for FET with graphene functionalized with azobenzne upon (a) UV light exposure: (*1*) functionalized graphene, (*2*) UV light exposure for 1 h, and (*3*) UV light exposure for long time; (b) visible light exposure: (*1*) functionalized graphene, (*2*) white light exposure for 1 h, and (*3*) white light exposure for long time; (c) energy level change upon UV and visible light exposure; (d) current change in FET devices with pristine graphene and functionalized graphene with azobenzene at 0V gate bias.

## EXPERIMENTAL

Monolayer graphene flakes were mechanically exfoliated onto Si substrate with 300 nm thermal oxide. We applied both optical contrast and Raman spectroscopy to identify the single-layer graphene (SLG) sheets. The 514 nm laser as an excitation source was used to avoid any damage or heating of graphene in the course of measuring. Exposure time was 10 s and the calibration was done using a reference Si peak positioned at 520 $cm^{-1}$.

Graphene channels patterned on a Si substrate with 300 nm thermal oxide were used for device fabrication by electron beam lithography (Nanobeam nB4, NBL), $O_2$ plasma, metal deposition [Cr (5 nm)/Au (50 nm)], and lift-off process. The channel of graphene FET was of 1 μm length and 2 μm width. The fabricated graphene FET device was functionalized by dipping it into a solution of azobenzene diazonium salt for 24 h followed by rinsing with acetone and dried in the atmosphere of $N_2$. Electrical characteristics of the FET device of pristine and functionalized graphene were estimated with a semiconductor parameter analyzer (4200-SCS, Keithley).

## CONCLUSIONS

We have demonstrated defect-free *p*-doping of graphene by its functionalization with covalently bonded azobenzene. The transformations between *cis* and *trans* structures induced by UV and visible light irradiation affected the electrical properties of graphene. There was observed the reversible light-modulated Dirac point of graphene upon exposure to UV and visible light. Analysis of transistor characteristics demonstrated that the charge carrier concentration could be modulated within $\pm 1 \times 10^{12}$ $cm^{-2}$ by UV and white light illumination via reversible photoisomerization of azobenzene while preserving mobility of pristine graphene. Retention of high mobilities, the ability to modulate doping by light and ease of processing of the azobenzene-graphene hybrids were advantageous over substitutional doping. Sensitivity of the graphene FET in detecting and amplifying relatively small changes in electrostatic potential due to molecular transformations was very high which presents a closer approach to doping control methods by using functionalization of graphene with photochromic molecules.

## REFERENCES


1. Bonaccorso, F., Sun, Z., Hasan, T., and Ferrari, A.C., *Nat Photonics.*, 2010, vol. 4, p. 611.
2. Bao, Q.L. and Loh K.P., *ACS Nano.,* 2012, vol. 6, p. 3677.
3. Avouris, P. and Xia, F.N., *MRS Bull.,* 2012, vol. 37, p. 1225.
4. Miao, X.C., Tongay, S., Petterson, M.K., Berke, K., Rinzler, A.G., and Appleton, B.R., *Nano Lett*., 2012, vol. 12, p. 2745.
5. Bae, S., Kim, H., Lee, Y., Xu, X.F., Park, J.S., and Zheng, Y., *Nat. Nanotechnol*., 2010, vol. 5, p. 574.
6. Konstantatos, G., Badioli, M., Gaudreau, L., Osmond, J., and Bernechea, M., Arquer, F.P.G.D., *Nat. Nanotechnol.,* 2012, vol. 7, p. 363.
7. Casiraghi, C., Hartschuh, A., Lidorikis, E., Qian, H., Harutyunyan, H., and Gokus, T., *Nano Lett.,* 2007, vol. 7, p. 2711.
8. Zhang. Y.B., Tang, T.T., Girit, C., Hao, Z., Martin, M.C., and Zettl, A., *Nature*, 2009, vol. 459, p. 820
9. Lee, E.J.H., Balasubramanian, K., Weitz, R.T., Burghard, M., and Kern, K., *Nat. Nanotechnol*., 2008, vol. 3, p. 486.
10. Mueller, T., Xia, F., Freitag, M., Tsang, J., and Avouris, P., *Phys. Rev. B,* 2009, vol. 79, p. 245430.
11. Xu, X.D., Gabor, N.M., Alden, J.S., Zvan, A.M.D., and Euen, P.L.M., *Nano Lett.*, 2010, vol. 10, p. 562.
12. Freitag, M., Low, T., Xia, F.N., and Avouris, P., *Nat. Photonics*., 2013, vol. 7, p. 53.
13. Castro, E.V., Novoselov, K.S., Morozov, S.V., Peres, N.M.R., Santos, J.M.B,, Nilsson, J., Guinea, F., Geim, A.K., and Castro Neto, A.H., *Phys. Rev. Lett.,* 2007, vol. 99, p. 216802.
14. Xia, F., Farmer, D.B., Lin, Y., and Avouris, P., *Nano Lett.,* 2010, vol. 10, p. 715.
15. Li, X., Wang, X., Zhang, L., Lee, S., and Dai, H., *Semiconductors Science*, 2008, vol. 319, p. 1229.
16. Bai. J., Zhong, X., Jiang, S., Huang, Y., and Duan, X., *Nat. Nanotechnol.,* 2010*,* vol. 5, p. 190.
17. Chen, J.H., Jang, C., Adam, S., Fuhrer, M.S., Willians, E.D., and Ishigami, M., *Nat. Phys.,* 2008, vol. 4, p. 377.
18. Guo, B., Liu, Q., Chen, E., Zhu, H., Fang, L., and Gong, J.R., *Nano Lett.,* 2010, vol. 10, p. 4975.
19. Wang, X., Li, X., Zhang, L., Yoon, Y., Weber, P.K., Wang, H., Guo, J., and Dai, H., *Science,* 2009*,* vol. 324, p. 768.
20. Wei, D., Liu, Y., Wang, Y., Zhang, H., Huang, L., Yu, G., *Nano Lett*., 2009, vol. 9, p. 1752.
21. Sun, Z., Yan, Z., Yao, J., Beitler, E., Zhu, Y., and Tour, J.M., *Nature,* 2010, vol. 468, p. 549.

22. Bekyarova, E., Itkis, M.E., Ramesh, P., Berger, C., Sprinkel, M., Heer, W.A., and Haddon, R.C., *J. Am. Chem. Soc.,* 2009, vol. 131, p. 1336.
23. Huang. P., Zhu, H., Jing, L., Zhao, Y., and Gao, X., *ACS Nano*, 2011, vol. 5, p. 7945.
24. Sinitskii, A., Dimiev, A., Corley, D.A,, Fursina, A.A., Kosynkin, D.V., and Tour, J.M., *ACS Nano*, 2010, vol. 4, p. 1949.
25. Evans, S.D., Johnson, S.R., Ringsdorf, H., Williams, L.M., and Wolf, H., *Langmuir*, 1998, vol. 14, p. 6436.
26. Ubukata. T., Hara, M., Ichimura, K., and Seki, T., *Adv. Mater.,* 2004, vol. 16, p. 220.
27. Hagen, R. and Bieringer, T., *Adv. Mater.,* 2001, vol. 13, p. 1805.
28. Schmidt, B., Sobotta, C., Malkmus, S., Laimgruber, S., Braun, M., and Zinth, W., *J. Phys. Chem. A,* 2004, vol. 108, p. 4399.
29. Feng, Y.Y. and Feng, W., *Opt. Mater.,* 2008, vol. 30, p. 876.
30. Simmons. J.M., In, I., Campbell, V.E., Mark, T.J., Leonard, F., and Gopalan, P., *Phys. Rev. Lett*., 2007, vol. 98, p. 086802.
31. Zhou, X.J., Zifer, T., Wong, B.M., Krafcik, K.L., Leonard, F., Vance, A.L., *Nano Lett*., 2009, vol. 9, p. 1028.
32. Ferrari, A.C., Meyer, J.C., Scardaci, V., Casiraghi, C., Lazzeri, M., Mauri, F., Piscanec, S., Jiang, D., Novoselov, K.S., Roth, S., and Geim, A.K., *Phys. Rev. Lett*., 2006, vol. 97, p. 187401.
33. Huang, P., Zhu, H.R., Jing, L., Zhao, Y.L., and Gao, X.Y., *ACS Nano*, vol. 5, p. 7945.
34. Zhang, H., Bekyarova, E., Huang, J.W., Zhao, Z., Bao, W.Z., Wang, F.L., Haddon, R.C., and Lau, C.N., *Nano Lett.,* vol. 11, p. 4047.
35. Fan, X.Y., Nouchi, R., and Tanigaki, K., *J. Phys. Chem. C*, 2011, vol. 115, p. 12960.
36. Kim, K., Lee, Z., Regan, W., Kisielowski, C., Crommie, M.F., and Zettl, A., *ACS Nano,* 2011, vol. 5, p. 2142.
37. Sharma, R., Baik, H., Perera, C.J., and Strano, M.S., *Nano Lett*., 2010, vol. 10, p. 398.
38. Niyogi, S., Bekyarova, E., Itkis, M.E., Zhang, H., Shepperd, K., Hicks, J., Sprinkle, M., Berger, C., Lau, C.N., De Heer, W.A., Conrad, E.H., and Haddon, R.C., *Nano Lett*., 2010, vol. 10, p. 4061.
39. Koehler, F.M., Jacobsen, A., Ensslin, K., Stampfer, C., and Stark, W.J., *Small*., 2010, vol. 6, p. 1125.
40. Sun, Z., Kohama, S.I., Zhang, Z., Lomeda, J.R., and Tour, J.M., *Nano Res*., 2010, vol. 3, p. 117.
41. Wu, Q., Wu, Y., Hao,Y., Geng, J., Charlton, M., Chen, S., Ren, Y., Ji, H., Li, H., Boukhvalov, D.W., Piner, R.D., Bielawski, C.W., and Ruoff, R.S., *Chem. Commun*., 2013, vol. 49, p. 677.